# DEVELOPMENT OF A CODE FOR A DIRECT NUMERICAL SIMULATION OF COMPRESSIBLE SHEAR FLOW INSTABILITIES

**Ricardo A. Coppola Germanos**
USP - Universidade de São Paulo
Escola de Engenharia de São Carlos - Departamento de Engenharia Aeronáutica
Av. Trabalhador São Carlense, 400 - SP - 13566-590, Brazil
gercop@sc.usp.br

**Marcello A. Faraco de Medeiros**
USP - Universidade de São Paulo
Escola de Engenharia de São Carlos - Departamento de Engenharia Aeronáutica
Av. Trabalhador São Carlense, 400 - SP - 13566-590, Brazil
marcello@sc.usp.br

***Abstract.*** *The engineering research and design requirements of today pose great challenges in computer simulation to engineers and scientists who are called on to analyze phenomena in continuum mechanics. The study of hydrodynamic instability is a subject well researched, seeking among other objectives, the development of propulsion systems based on supersonic combustion. In the current work, the instability of the compressible free shear layer at relatively low Reynolds number was investigated. In the aerospace context, important applications involve compressible flows at relatively low Reynolds number. Among them, the flow on gas turbine blades and the flow on high lift devices such as slats and flaps at high angle of attack are particularly important. In aerodynamic applications in low Reynolds number, often a substantial portion of the flow is in the transition regime, or in the initial stages of a turbulent flow. Despite the extensive research carried out in the field, there are various aspects of the transition process that require further studies. The transition in compressible flow is an example. In this work the simulation of compressible Navier-Stokes equations were performed. The spatial derivatives of these equations were discretized through of the high-order finite difference method. To solve the temporal derivatives the high-order Runge-Kutta method was adopted. Firstly, an analysis of the amplification rate in linear regime was performed in order to verify the numerical code. Tests were also performed in the nonlinear regime of two-dimensional waves and it was possible to reproduce the vortex roll up and pairing. Finally the initial results with the three-dimensional equations were presented.*

***Keywords:*** *Numerical methods, Compact differences schemes, Hydrodynamic instability, Compressible flows, free shear layer phenomenon and Linear Theory*

## 1. Introduction

The study of transition to turbulence in incompressible mixing layer has constituted one of the main research themes in turbulence in the last ones thirty years. The mixing layer is a fundamental flow that it comes in numerous practical situations such as aerodynamics, combustion, environmental engineering, etc. A mixing layer develops starting from the interface of two-stream of different speeds. The profile of velocity formed possesses an inflection point that is unstable to infinitesimal disturbances. This instability is inviscid and it is called Kelvin-Helmholtz instability. It is responsible for the formation of structures of vorticity guided in the lateral sense. This behavior was evidenced in experiences of laboratory carried out by Birch and Eggers (1973) and Brown and Roshko (1974). According to Lesieur (1997) due to the vorticity concentration, to the recognizable form and the unpredictability in relation to the location in the time and space, these vorticity structures present all the characteristics for they are considered as coherent structures.

Besides the Kelvin-Helmholtz vortex, many experimental works presented by Bernal and Roshko (1986), Huang and Ho (1990) and numerical works published by Lin and Roebucks (1984), Metcalfe et al. (1987) put in evidence the existence of one secondary instability, that causes in the stagnation area between the Kelvin-Helmholtz vortex, intense longitudinal counter-rotative vortex. The longitudinal vortex, denominated hairpins are easily identifiable in a traverse cut for the form in mushroom. In the transitional and turbulent flows, the primary and secondary vortexes are responsible for the largest portion of the transfer of conservation of mass, momentum and energy, respectively.

Studies of the linear stability of compressible mixing layer presented by Lessen, Fox and Zien (1966), Blumen, Drazin and Billings (1975) show a strong reduction in the amplification rate of two-dimensional disturbances in the flow as Mach number is increased. In compressible mixing layer there are two flows of different speeds and therefore with two characteristics Mach number. In this case the representative parameter is denominated convective Mach number (Papamoschou and Roshko, 1988). Experiments show that this parameter characterizes the flow correctly for $Ma < 0.6$. Simulations carried out by Sandham and Reynolds (1990,1991) show that for convective Mach number lower than $0.6$ the two-dimensional disturbances is the most rapidly amplified whilst for convective Mach number above to $0.6$, the oblique

waves are dominant and the mixing layer will have a strongly three-dimensional structure.

These kinds of flows possess wide range of space and time scales and therefore, it requires high accuracy in the numerical solution. This requirement of accuracy can be achieve by the use of spectral methods (Canuto et al., 1987). The use of this scheme is restricted to flows in simple domains and simple boundary conditions. In order to overcome these difficulties an alternative numerical representations can be used, as the finite differences schemes and the finite volume Schemes. The finite differences schemes is justified by the possibility of the use of more general boundary conditions, although the schemes with high order of accuracy is also restricted to the problem with simple domains. The advantage of these schemes in relation to finite volume schemes is that high-order approximations can be used. The finite volume schemes has advantages in working with complex domains and also with complex boundary conditions. The finite difference schemes may be classified as explicit or implicit. According to Mahesh (1998), implicit schemes are significantly more accurate for the small scales than explicit schemes with the same stencil width. The implicit schemes are extremely attractive when explicit time advancement schemes are used.

In the present work, a high-order compact scheme was adopted to solve the spatial derivatives (Lele, 1992). The computational domain is periodic in x and z direction. In the y-direction, the free-slip condition was adopted according Medeiros et al. (2000) and Souza (2003). This boundary condition should produce accurate results for a sufficient large distance from the mixing layer. Another possibility is to use an exponential decay, except that this method is only rigorously correct in the linear regime. Thompson (1987) presents non-reflecting boundary conditions. The idea of these boundary conditions is to consider the characteristic form of the Euler equation at the boundary. Finally, in order to solve the temporal derivatives another method was adopted. In agreement with Williamson (1980), the time-advance is obtained by a high-order Runge-Kutta scheme. This scheme is conditionally stable. In order to simulate these phenomena appropriately is necessary to use small time increments in the numerical simulation to assure that the criterion of stability was satisfied. Therefore the restrictions of stability are only two: that due to convection and due to the diffusion. Kloker (1993) used this same scheme.

The linear and non-linear evolution of two- and three-dimensional instability waves in the unconfined mixing layer was simulated. Tests based on the linear stability theory were used to validate the code. In this tests, the growth rate obtained in simulations was compared with others numerical and experimental works. Simulations in non-linear regime also were performed. All this tests are related to the temporal instability of a parallel mixing layer. Emphasize that the objective of this work to the long time consists in the simulation of compressible boundary layer phenomenon, and therefore, the authors of this work consider very important a verification of the code with some problems more simplified, as it is the case of mixing layer problem. Other tests were performed with the simulation of the linear acoustic wave problem (Germanos, Medeiros and Souza, 2004a, 2004b).

The organization of the paper is as follows. Section 2 presents the formulation adopted in the current work. The details of the numerical method and boundary conditions are described in the section 3. Section 4 shows a numerical simulation of the mixing layer phenomena. The last section presents the conclusion of this work.

## 2. Formulation

In this study, the governing equations are the compressible, three-dimensional Navier-Stokes equations according to Sandham and Reynolds (1991) and Eibler (1996). They consist of the momentum equations for the velocity component ($u$,$v$,$w$) in the streamwise direction (x), normal direction (y) and spanwise direction (z)

$$\frac{\partial \rho u_i}{\partial t} + \frac{\partial \rho u_i u_j}{\partial x_j} = -\frac{\partial p}{\partial x_i} + \frac{\partial \tau_{ij}}{\partial x_j}, \tag{1}$$

and the continuity equation

$$\frac{\partial \rho}{\partial t} + \frac{\partial \rho u_j}{\partial x_j} = 0, \tag{2}$$

where $x_i$ are the Cartesian coordinates ($x$,$y$,$z$), $t$ is the time, $u_i$ are the velocity components ($u$,$v$,$w$), $\rho$ is the density and $p$ is the pressure. The non-dimensional constitutive relations for a Newtonian fluid is

$$\tau_{ij} = \frac{1}{Re}\left(\frac{\partial u_i}{\partial x_j} + \frac{\partial u_j}{\partial x_i} - \frac{2}{3}\frac{\partial u_k}{\partial x_k}\delta_{ij}\right). \tag{3}$$

These equations were defined with the following non-dimensionalization scheme

$$u_i = \frac{u_i^*}{V_\infty^*}, \quad \rho = \frac{\rho^*}{\rho_\infty^*}, \quad p = \frac{p^*}{\rho_\infty^* V_\infty^{*2}}, \quad t = \frac{t^* V_\infty^*}{\delta_{\omega_0}^*}, \quad x_i = \frac{x_i^*}{\delta_{\omega_0}^*}, \quad \alpha = \alpha^* \delta_{\omega_0}^*, \quad \omega = \frac{\omega^* \delta_{\omega_0}^*}{V_\infty^*}, \tag{4}$$

where $V_\infty^*$ is the free stream velocity, $\rho_\infty^*$ is the free stream density, $\alpha^*$ is the wavenumber of the disturbed flow, $\omega^*$ is the frequency of the flow and $\delta_{\omega_0}^*$ is the vorticity thickness of the initial velocity given by

$$\delta_{\omega_0}^* = \frac{U_1^* - U_2^*}{|d\bar{u_0}^*/dy^*|_{max}}, \tag{5}$$

where the subscript 1 e 2 refers to the upper $(y > 0)$ and lower $(y < 0)$ free stream, respectively. The Reynolds number of the flow are defined by

$$Re = \frac{\rho^*_\infty \, V^*_\infty \, \delta^*_{\omega_0}}{\mu^*}, \tag{6}$$

where $\mu^*$ is the dynamic viscosity.

In the actual stage, an isentropic flow hypothesis was adopted (Sullivan, 1981). Therefore, the equation of the perfect gases combined with to the equation of energy can be written in the following way

$$p = \left( \frac{p^*_0}{\rho^*_\infty \, V^{*2}_\infty} \right) \rho^\gamma, \tag{7}$$

where $p^*_0$ is the mean flow pressure and $\gamma = c_p/c_v$ is the relation of the specific heat.

## 3. Numerical Method

This section presents the numerical method adopted for a time-developing free shear layer problem. In order to solve the spatial derivatives, the implicit schemes also called compact finite-difference schemes were adopted. The finite-difference approximation to the derivative of the function is expressed as a linear combination of the given function values on a set of nodes. First, a uniformly spaced mesh was considered where at the nodes is $x_i = ih$ for $0 \leq i \leq N$. In compact finite-difference schemes the value of $f'_i$ possess a dependence with all the values of nodes. These compact schemes are classified as implicit. Collatz (1966) and Kopal (1961) show that implicit schemes are significantly more accurate for short length scales than explicit schemes. This increase of accuracy is reached being inverted a tridiagonal matrix to obtain the derivative values. Strang (1988), presents quite efficient methods to solve this kind of linear system. Lele (1992) emphasizes the importance of using methods of high-order and proposes a schemes with $3^{rd}$ order approximation at the boundaries, a $4^{th}$ order approximation for points near the boundaries and $6^{th}$ order approximation in the interior of the mesh.

The $6^{th}$ order compact finite-difference schemes was adopted in this work to solve the spatial derivatives. In longitudinal and spanwise directions the periodic boundary condition was used, while in the normal direction a free-slip condition was adopted as

$$v = 0, \tag{8}$$

$$\frac{\partial}{\partial y}(u, w, p, \rho) = 0. \tag{9}$$

The free shear layer problem develops from specified initial conditions shown by Fortune (2000). Hyperbolic tangent mean profile was used

$$\bar{u_0}(y) = \left( \frac{U^*_1 - U^*_2}{2} \right) \tanh(2y), \tag{10}$$

where $U^*_1$ and $U^*_2$ are the upper $(y > 0)$ and the lower $(y < 0)$ free stream. Along with the velocity profile the disturbance flow were defined as

$$u' = \frac{2\sigma y}{(\alpha_1 \alpha_2)} \left[ A_1 \sin(\alpha_1 x)\alpha_2 + A_2 \sin(\alpha_2 x)\alpha_1 \right] \exp(-\sigma y^2), \tag{11}$$

$$v' = \left[ A_1 \sin(\alpha_1 x) + A_2 \sin(\alpha_2 x) \right] \exp(-\sigma y^2), \tag{12}$$

$$w' = 0, \tag{13}$$

$$\rho' = 0, \tag{14}$$

$$p' = 0, \tag{15}$$

where $A$ is the amplitude, $\alpha$ is the wavenumber and $\sigma$ is the spread of the disturbance in the y-direction. The subscript 1 refers to the dominant mode and subscript 2 refers to the subharmonic excitation. Uniform density is assumed for the initial mean flow and the mean pressure is obtained by the equation 7.

Bellow the discretization used in the streamwise, normal and spanwise direction are present. The letter $i, j, k$ represents the grid position in $x$, $y$ and $k$ direction, which varies from 0 to $M, N, P$ respectively. In the x-direction, since it is analogous for the z-direction, the $6^{th}$ order implicit (compact) derivatives for $0 < i < M$ as follows

$$\begin{bmatrix} 3 & 1 & & & & & 1 \\ 1 & 3 & 1 & & & & \\ & \ddots & \ddots & \ddots & & & \\ & & 1 & 3 & 1 & & \\ & & & \ddots & \ddots & \ddots & \\ & & & & 1 & 3 & 1 \\ 1 & & & & & 1 & 3 \end{bmatrix} \begin{bmatrix} f'_{0,j,k} \\ f'_{1,j,k} \\ \vdots \\ f'_{i,j,k} \\ \vdots \\ f'_{M-1,j,k} \\ f'_{M,j,k} \end{bmatrix} = \begin{bmatrix} \frac{1}{12dx}(f_{M-1,j,k} + 28f_{M,j,k} - 28f_{1,j,k} - f_{2,j,k}) \\ \frac{1}{12dx}(f_{M,j,k} + 28f_{0,j,k} - 28f_{2,j,k} - f_{3,j,k}) \\ \vdots \\ \frac{1}{12dx}(f_{i+2,j,k} + 28f_{i+1,j,k} - 28f_{i-1,j,k} - f_{i-2,j,k}) \\ \vdots \\ \frac{1}{12dx}(f_{M-3,j,k} + 28f_{M-2,j,k} - 28f_{M,j,k} - f_{0,j,k}) \\ \frac{1}{12dx}(f_{M-2,j,k} + 28f_{M-1,j,k} - 28f_{0,j,k} - f_{1,j,k}) \end{bmatrix}.$$

In the normal direction, a non-periodic scheme was adopted. This scheme was used by Souza et al. (2002). At the boundaries a $5^{th}$ order asymmetric approximation was proposed, whilst for points near the boundaries a $6^{th}$ order asymmetric approximation was used. For the interior points, a $6^{th}$ order symmetric approximation was adopted whereas this scheme satisfies the equation 8). Therefore the $6^{th}$ order implicit (compact) derivatives for $0 < i < N$ adopted was

$$\begin{bmatrix} 1 & 4 & & & & & \\ 1 & 6 & 2 & & & & \\ & \ddots & \ddots & \ddots & & & \\ & & 1 & 3 & 1 & & \\ & & & \ddots & \ddots & \ddots & \\ & & & & 2 & 6 & 1 \\ & & & & & 4 & 1 \end{bmatrix} \begin{bmatrix} f'_{i,0,k} \\ f'_{i,1,k} \\ \vdots \\ f'_{i,j,k} \\ \vdots \\ f'_{i,N-1,k} \\ f'_{i,N,k} \end{bmatrix} =$$

$$\begin{bmatrix} \frac{1}{24dy}(-74f_{i,0,k} + 16f_{i,1,k} + 72f_{i,2,k} - 16f_{i,3,k} + 2f_{i,4,k}) \\ \frac{1}{120dy}(-406f_{i,0,k} - 300f_{i,1,k} + 760f_{i,2,k} - 80f_{i,3,k} + 30f_{i,4,k} - 4f_{i,5,k}) \\ \vdots \\ \frac{1}{12dy}(f_{i,j+2,k} + 28f_{i,j+1,k} - 28f_{i,j-1,k} - f_{i,j-2}, k) \\ \vdots \\ \frac{1}{120dy}(406f_{i,N,k} + 300f_{i,N-1,k} - 760f_{i,N-2,k} + 80f_{i,N-3,k} - 30f_{i,N-4,k} + 4f_{i,N-5,k}) \\ \frac{1}{24dy}(74f_{i,N,k} - 16f_{i,N-1,k} - 72f_{i,N-2,k} + 16f_{i,N-3,k} - 2f_{i,N-4,k}) \end{bmatrix}.$$

The schemes above was modified to work with the equation 9 as proceeds bellow

$$\begin{bmatrix} 1 & & & & & & \\ 1 & 6 & 2 & & & & \\ & \ddots & \ddots & \ddots & & & \\ & & 1 & 3 & 1 & & \\ & & & \ddots & \ddots & \ddots & \\ & & & & 2 & 6 & 1 \\ & & & & & & 1 \end{bmatrix} \begin{bmatrix} f'_{i,0,k} \\ f'_{i,1,k} \\ \vdots \\ f'_{i,j,k} \\ \vdots \\ f'_{i,N-1,k} \\ f'_{i,N,k} \end{bmatrix} =$$

$$\begin{bmatrix} 0.0 \\ \frac{1}{120dy}(-406f_{i,0,k} - 300f_{i,1,k} + 760f_{i,2,k} - 80f_{i,3,k} + 30f_{i,4,k} - 4f_{i,5,k}) \\ \vdots \\ \frac{1}{12dy}(f_{i,j+2,k} + 28f_{i,j+1,k} - 28f_{i,j-1,k} - f_{i,j-2}, k) \\ \vdots \\ \frac{1}{120dy}(406f_{i,N,k} + 300f_{i,N-1,k} - 760f_{i,N-2,k} + 80f_{i,N-3,k} - 30f_{i,N-4,k} + 4f_{i,N-5,k}) \\ 0.0 \end{bmatrix}.$$

Time-advance of the computational variables ($\rho$,$\rho u_i$) is obtained by the $4^{th}$ order Runge-Kutta method. The discretized transport equations are used to determine the values of the variables at each point of the computational domain at time $t_{n+1} = t_n + dt$. The schemes here described works in 4 steps (Ferziger, 1997)

$$f^*_{n+\frac{1}{2}} = f_n + \frac{dt}{2} f(t_n, f_n), \tag{16}$$

$$f^{**}_{n+\frac{1}{2}} = f_n + \frac{dt}{2} f(t_{n+\frac{1}{2}}, f^*_{n+\frac{1}{2}}), \tag{17}$$

$$f^*_{n+1} = f_n + dt f(t_{n+\frac{1}{2}}, f^{**}_{n+\frac{1}{2}}), \tag{18}$$

$$f_{n+1} = f_n + \frac{dt}{6}[f(t_n, f_n) + 2f(t_{n+\frac{1}{2}}, f^*_{n+\frac{1}{2}}) + 2f(t_{n+\frac{1}{2}}, f^{**}_{n+\frac{1}{2}}) + f(t_{n+1}, f^*_{n+1})]. \tag{19}$$

The first two steps, Eq. 16 and 17 use a formulation of Euler "predictor" explicit and a formulation of Euler "corrector" implicit for the same time $t + dt/2$. The following step (18) is a "predictor" based on the rule of the medium point for the whole step $(t + dt)$ and the last (19), "corrector" is based on Simpson's rule. The combination of these steps results in a $4^{th}$ order accuracy algorithm.

## 4. Numerical Results

In this section, results from direct numerical simulations of the compressible Navier-Stokes equations are used to show physics of vorticity transport in linear and non-linear regime of the time-developing mixing layer problem. It was carried out the analysis of the amplification rate in linear regime for an inviscid and viscous flows and the growth rate was compared with other numerical results. In the non-linear regime, first, it was simulated a flow using a small disturbance of a stipulated mode. After, it was selected a small disturbances composed by a dominant and a subharmonic mode to reproduce the secondary instability. Finally the initial steps to simulation of three-dimensional problem were presented.

In this work the high-order compact finite-difference schemes was used to solve spatial derivatives. Details about this method was given in section 3. The initial condition was also specified in this section. The boundary condition in the y-direction was free-slip. Ideally, one would like enforcing a vanishing perturbation velocity at a very large distance from the shear layer, but that requires very large computational domain. For a sufficient large distance form shear layer, the free-slip boundary condition should produce accurate results. In longitudinal and spanwise direction a periodic boundary condition was enforced. An important aspect to be considered in these simulations is the treatment of the vertical diffusion. This diffusion increases the width of the free shear layer during the simulation, which implies in a variation of the mean flow. Thus, there should be a variation of the amplification rate, even in the linear regime. The strategy adopted here, to avoid this diffusion, was to cancel the vertical diffusions terms.

One of the objectives of this work is to analyze the variation of the amplification rate of the disturbances. Thus the variables were decomposed in two parts: temporary mean and small disturbance. This way the primitive variables can be written in the following way

$$\begin{aligned}
u(x,y,z,t) &= u_0(y) + u', \\
v(x,y,z,t) &= + v', \\
w(x,y,z,t) &= + w', \\
\rho(x,y,z,t) &= \bar{\rho_0} + \rho', \\
p(x,y,z,t) &= \bar{p_0} + \rho'.
\end{aligned} \tag{20}$$

where the subscript $(_0)$ refers to a temporary mean flow and $(')$ refers to a small disturbance. The mean flow is invariant in the longitudinal and spanwise direction and the components $(v, w)$ of mean velocity is null. For the time-developing mixing-layer problem the temporal analysis was performed, in other words disturbances grow in time and not in space. Thus, the wavenumber $\alpha$ and $\beta$ are real quantities. The streamwise wavelength of a disturbance is given by $L_x = 2\pi/\alpha$ and the amplification rate by $\omega_i$.

The first step was the simulation of the compressible Euler equations for a two-dimensional flow in linear regime. The objective of this simulation was to compare the growth rate of the two-dimensional disturbances with other numerical works. The mesh begun with dimension of $40 \times 100$, number of points in x and y direction. The initial amplitude of the disturbance was approximately $10^{-8}$. The results presented here correspond to regime governed by the linear theory. Figure 1 shows the growth rate of unstable waves at various Mach number as a function of wavenumber $\alpha$. The theoretical results used in this paper was obtained through the temporal linear stability analysis carried out by Sandham and Reynolds, 1991. The dashed-dotted line is the computational result that shows a growth rate at Mach number equals to $0.01$. The circle symbol gives the theoretical results from a incompressible theory. It is important to mention that this simulation could not be performed at Mach number below $0.4$, because of convergence problems related to the simulation

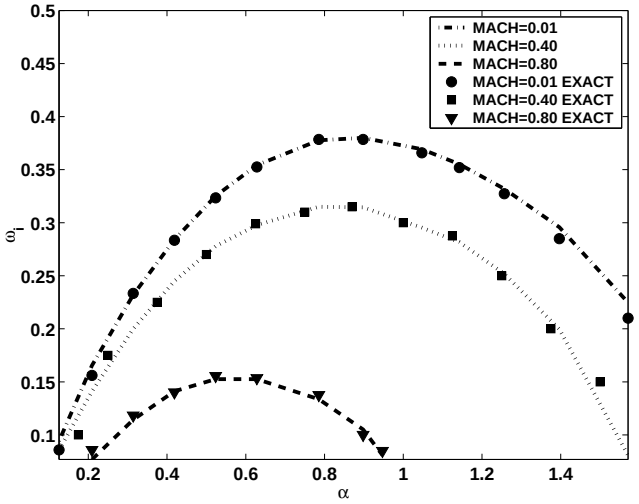


Figure 1. Amplitude evolution from two-dimensional inviscid flow with temporal linear instability analysis.

of incompressible flows with a compressible formulation. In simulation of a compressible flow at Mach number equals to $0.4$ we can observed that the maximum amplification rate represented by the dotted line decreased to approximately $0.3$. The numerical result is also consistent to the theoretical analysis as it can be seen by the square symbol. In the curve at Mach number equals $0.8$ represented by dashed lines, the decrease of the amplification rate becomes more visible approaching of $42\%$ of the value for the incompressible flow. The diamond symbol is the prediction from a compressible flow at Mach number equals $0.8$. Based on these results, we can be confirmed in agreement with other works that the amplification rate of these waves is strongly reduced as Mach number increases.

The simulation of the compressible Navier-Stokes equations for a two-dimensional flow was also performed. For this problem the initial amplitude of the disturbance was approximately $10^{-6}$. The wavenumber $\alpha$ of the disturbance selected for the simulation was $\pi/16 = 0.89$. This is close to the wavenumber of maximum amplification. Figures from 2 to 5 show the evolution of the amplification rate as a function of non-dimensional time. The vertical coordinate is in logarithm scale. In this figure there is a region of exponential amplification that corresponds to the regime governed by the linear theory.

Figure 2 shows the amplitude evolution of a viscous flows at Mach number equals to $0.01$ and Reynolds number equals to $160$. The amplification rate obtained in simulation was approximately to $0.34$. Numerical results reproduced by Fortuné (1992) shows a amplification rate around to $0.31$. The same behavior can be seen in figure 3 for Reynolds number of $400$. Here the computational amplification rate is approximately to $0.36$, while the growth rate obtained by Fortuné (1992) is about to $0.34$. In these cases the amplification rate obtained numerically is overestimates but the disagreement could be attributed to a hypothesis for an isentropic flow assumed in the present work.

Figure 4 presents the amplification rate for Mach number equals $0.4$ and Reynolds number equals $500$. The amplification rate obtained in this simulation was $0.30$. Numerical results carried out by Sandham and Reynolds (1991) give an amplification rate about $0.28$. Last, figure 5 shows the simulation for Reynolds number equals to $1600$. In this case the amplification rate found was approximately to $0.30$. This amplification rate compared favorably with linear stability theory.

The next simulations were carried out in non-linear regime. In these simulations the vertical diffusion was included. The initial amplitude of the disturbance was approximately $10^{-4}$. First, the disturbance was composed by only one mode with wavenumber $\alpha = \pi/4$. Figure 6 shows the sequence of the evolution of disturbances in time. It can be observed that the disturbance thickness increases until the limit cycle oscillation. Figure 7 shows the two-dimensional evolution in time of the disturbance composed by two modes: $\alpha_1 = \pi/4$ (dominant mode) and $\alpha_2 = \alpha_1/2 = \pi/2$ (subharmonic mode). In this sequence it was possible to reproduce the vortex roll up and pairing. Figure 8 shows the results for the three-dimensional problem. Emphasizes that the results presented in this work correspond the first simulations carried out with the three-dimensional problem.

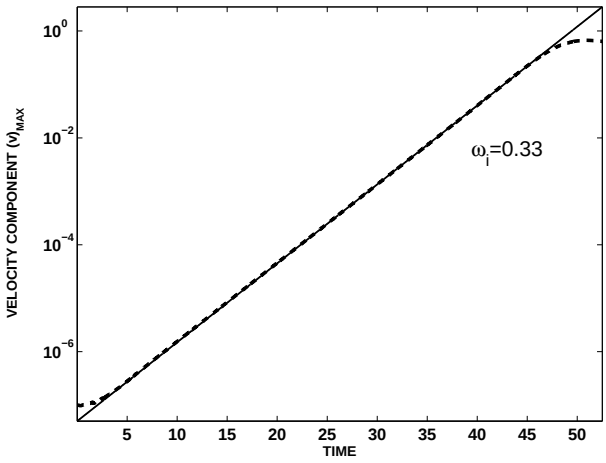


Figure 2. Amplitude evolution from viscous flow at Mach number equals to $0.01$, Reynolds number equals to $160$ and wavenumber approximately to $0.89$.

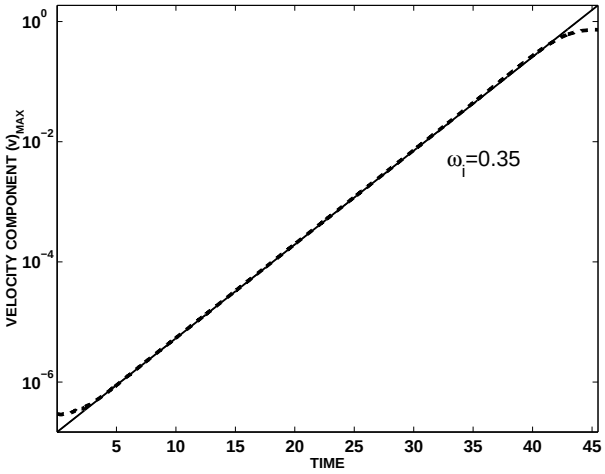


Figure 3. Amplitude evolution from viscous flow at Mach number equals to $0.01$, Reynolds number equals to $400$ and wavenumber approximately to $0.89$.

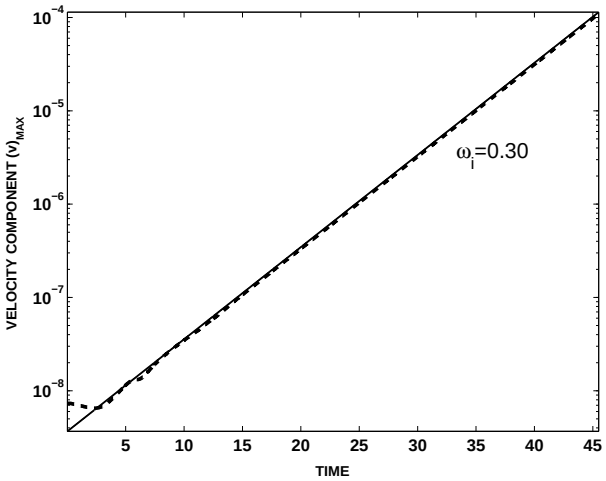


Figure 4. Amplitude evolution from viscous flow at Mach number equals to $0.4$, Reynolds number equals to $500$ and wavenumber approximately to $0.39$.

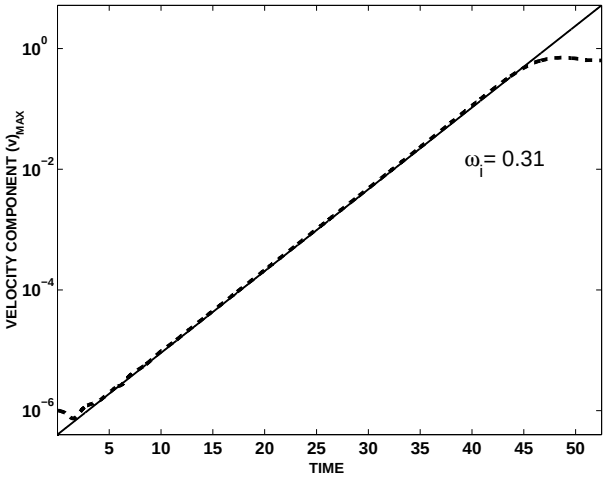


Figure 5. Amplitude evolution from viscous flow at Mach number equals to $0.4$, Reynolds number equals to $1600$ and wavenumber approximately to $0.39$.

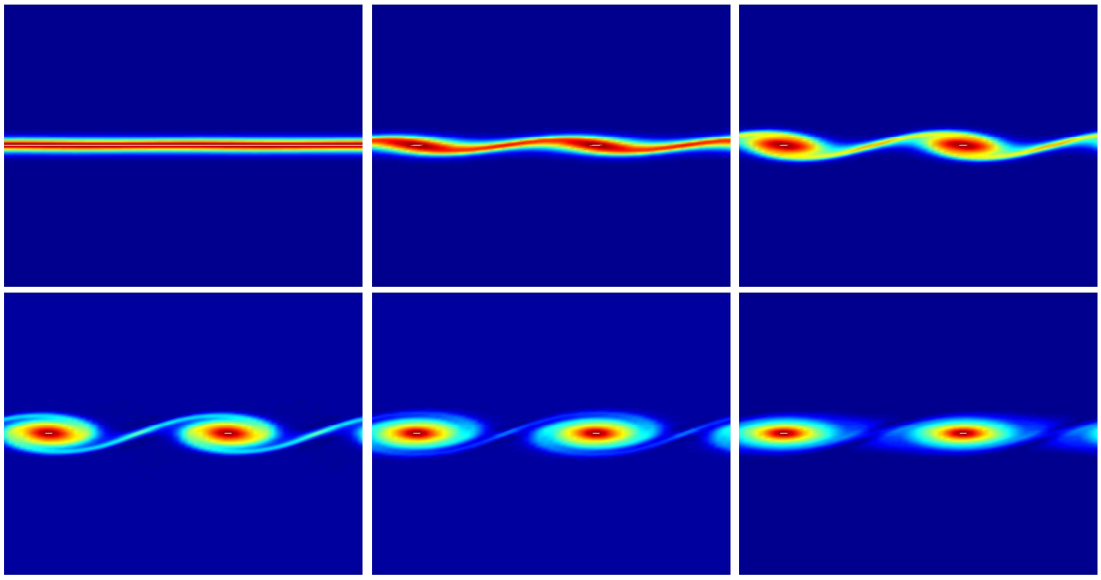

Figure 6. The linear and nonlinear two-dimensional evolution of disturbance composed of only mode. The frames presented correspond to the non-dimensional times 0.37, 0.45, 0.47, 0.50, 0.52 and 0.55.

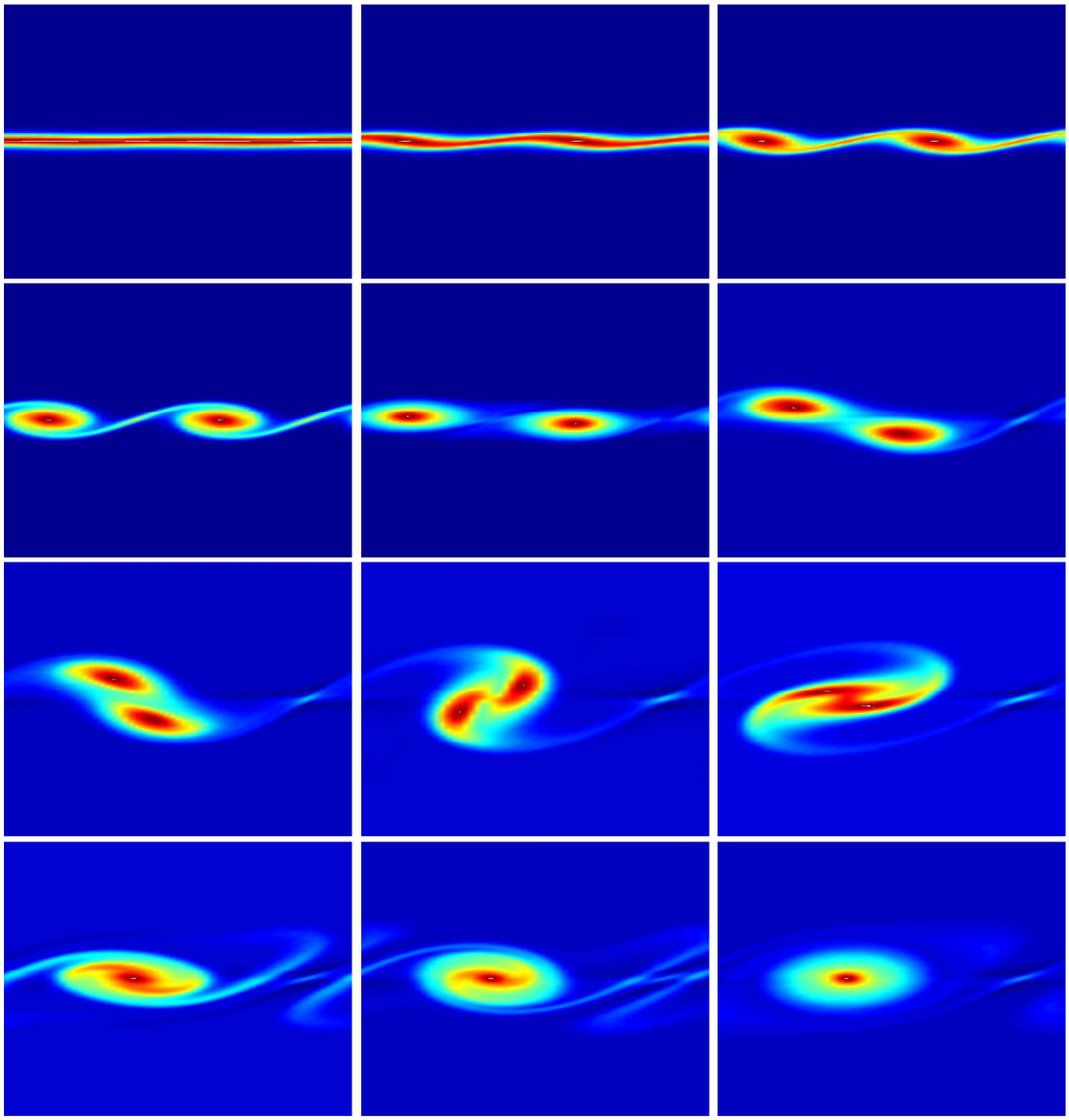

Figure 7. The linear and nonlinear two-dimensional evolution of disturbance composed of a dominant mode and a sub-harmonic seed. The frames presented correspond to the non-dimensional times 0.30, 0.35, 0.37, 0.40, 0.47, 0.52, 0.55, 0.57, 0.60, 0.65, 0.67 and 0.77

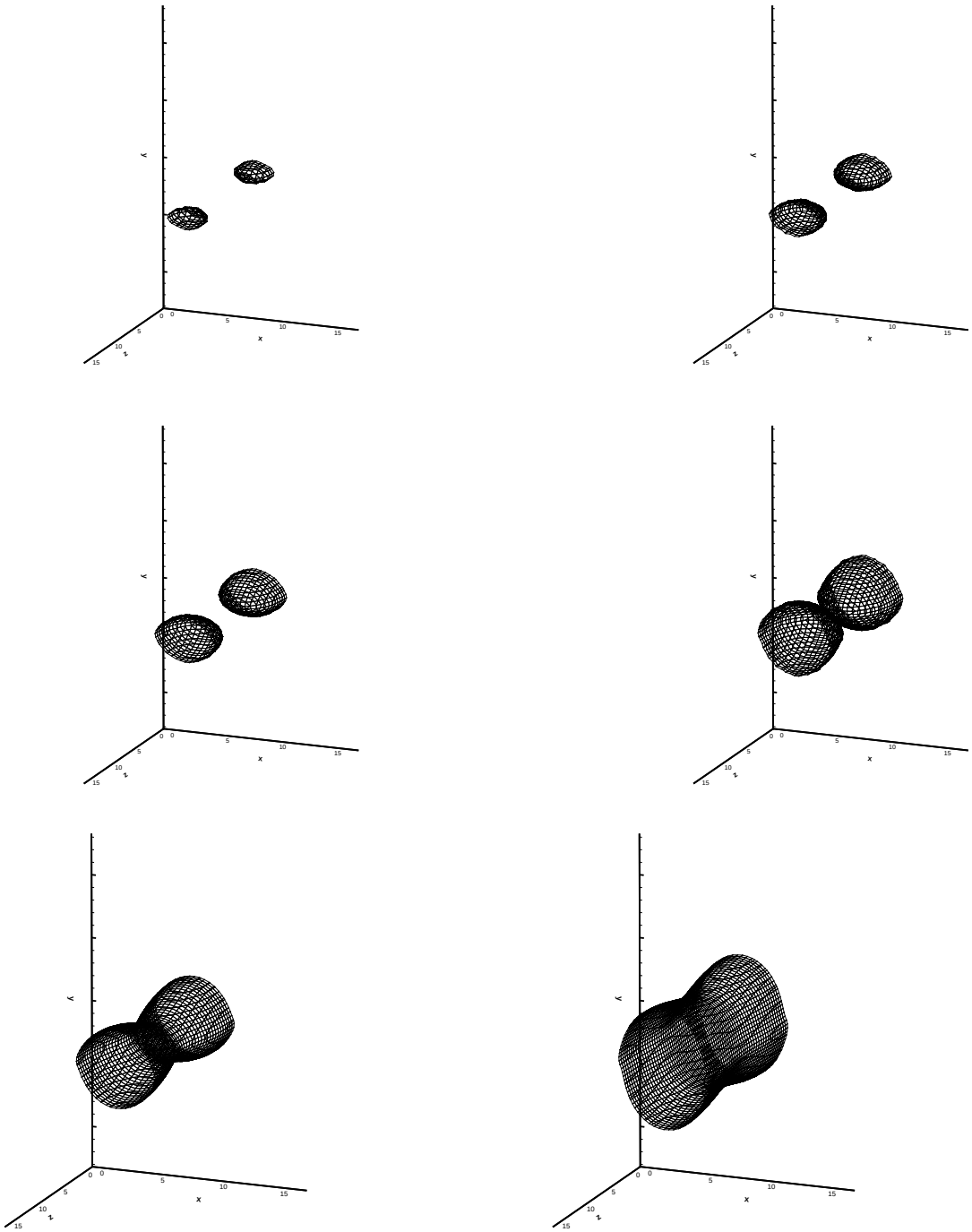

Figure 8. The linear and nonlinear three-dimensional evolution of disturbance composed of a dominant mode. The frames presented correspond to the non-dimensional times 0.11, 0.23, 0.38, 0.68, 0.80 and 1.0.

## 5. Conclusions

In this work the numerical simulation of a free shear layer problem was performed. The governing equations were the compressible Navier-Stokes equations for a isentropic flow. The $6^{th}$ order compact finite-difference schemes was used for solve the spatial derivatives. The method adopted was accurate in time, using a $4^{th}$ order Runge-Kutta scheme. The free-slip boundary condition was used and the results were very satisfactory.

The compressible shear layer flow was simulated giving some interesting results. In the linear regime was possible to obtain an good amplification rate. From the discussion above it appears that the isentropic flow hypothesis provides an interesting approach for simulation this problem. The numerical simulation carried out for viscous flows presented a small difference in the amplification rate compared to the other numeric works. The disagreement could be attributed to a difference in formulation adopted. In this work the viscosity of the fluid was assumed constant, whilst other works assume that the viscosity varies with the temperature.

For simulations in non-linear regime the results were interesting and it was possible reproduce some phenomenon. First, it was presented the evolution of disturbance composed of a dominant mode. Later it was introduced a subharmonic mode, and this way, it was possible to reproduced the secondary instability. The results for all cases with the free shear layer problem were satisfactory. The author considered important to carried out more test with the three-dimensional problem. Future works will present more detailed analysis of this three-dimensional phenomenon.

## 6. Acknowledgments

The financial support from FAPESP (State of Sao Paulo Research Support Foundation) – Grant number 02/09256-3 is greatly acknowledged.

## 7. References

Bernal L. and Roshko A.,1986, "Streamwise vortex structure in plane mixing ", J. Fluid Mech., pp. 429-525.

Birch, S. F. and Eggers J. M.,1973, "A critical review of the experimental data for developed free turbulent shear layers.", NASA SP-321, pp. 11-40.

Blumen, W., Drazin, P. G. and Billings D. F.,1975, "Shear layer instability of an inviscid compressible fluid. Part 2", J. Fluid Mech., Vol. 71, pp. 305-316.

Brown G. L. and Roshko A.,1974, "On density effects and large scale structure in turbulent mixing layers", J. Fluid Mech., Vol. 64, pp. 775-816.

Canuto C., Hussaini M. Y., Quarteroni A. and Zang T. A.,1987, "Spectral Methods in Fluid Dynamics".

Collatz L.,1966, "The numerical treatment of differential equations". Springer-Verlag, New York.

Eibler, W. and Bestek, H.,1996, "Spatial numerical simulations of linear and weakly nonlinear wave instabilities in supersonic boundary layers", Theoretical and Computational Fluid Dynamics, Vol. 8, pp. 219-235.

Ferziger J. H. and Peric M.,1997, "Computational methods for fluid dynamics", Springer.

Fortuné V.,1992, "Étude par simulation numérique directe du rayonnement acoustique de couches de mélangue isothermes et anisothermes.", PhD thesis, Université de Poitier.

Germanos R. A. C., Medeiros, M. A. F. and Souza, L. F.,2004, "Development of a computational code for studying compressible shear layer flow", "IV Escola de Primavera em TransiÃğÃčo e TurbulÃłncia".

Germanos R. A. C., Souza, L. F. and Medeiros, M. A. F.,2004, "Analysis of dispersion errors in acoustic wave simulations", "$10^{th}$ Brazilian Congress of Thermal Sciences and Engineering".

Huang L. and Ho C.,1988, "Small-scale transition in a plane mixing layer", Ann. Rev. Fluid Mech., Vol. 20, pp. 487-526.

Kloker, M., Rist, R. and Fasel, H.,1993, "Outflow boundary conditions for spatial Navier-Stokes simulations of boundary layer transition.", AIAA J., Vol. 31, pp. 620-628.

Kopal Z.,1961, "Numerical Analysis". Wiley, New York.

Lele S. K.,1990, "Compact finite difference schemes with spectral-like resolution.", J. Comput. Physics, Vol. 103, pp. 16-42.

Lesieur M.,1997, "Turbulence in fluids", Kluwer Academic Publisher, third edition.

Lessen M., Fox, J. A. and Zien, H. M., 1966, "Stability of the laminar mixing of two parallel streams with respect to supersonic disturbances", J. Fluid Mech., Vol. 25, pp. 737-742.

Medeiros, M. A. F., Silvestrini, J. H. and Mendonça, M. T.,1990, "Using linear and non-linear stability theory for evaluating code accuracy.".

Mahesh, K.,1998, "A family of high order finite difference schemes with good spectral resolution.", J. Comput. Physics, Vol. 142, pp. 332-358.

Metcalfe, R., Orzag, S., Brachet M., Menon S. and Riley, J.,1987, "Secondary instability of a temporally growing mixing layer.", J. Fluid Mech.

Papmoschou, D. and Roshko, A.,1988, "The compressible turbulent shear layer: An experimental study.", J. Fluid Mech.,

Vol. 197, pp. 453-477.

Sandham, N. D. and Reynolds, W. C.,1990, "Compressible mixing layer: Linear theory and direct simulation.", AIAA Journal, Vol. 28, No. 4, pp. 618-624.

Sandham, N. D. and Reynolds, W. C.,1991, "Three-dimensional simulations of large eddies in the compressible mixing layer.", J. Fluid Mech., Vol. 224, pp. 133-158.

Strang, G.,1988, "Linear Algebra and its applications."

Souza, L. F., 2003, "Instabilidade centrífuga e transição para turbulência em escoamentos laminares sobre superfície côncava.", PhD thesis, Instituto Tecnológico de Aeronaútica.

Souza, L. F., Mendonça, M. T. and Medeiros, M. A. F.,2002, "Assessment of different numerical schemes and grid refinement for hydrodinamic stability simulations.", $9^{th}$ Brazilian Congress of Thermal Sciences and Engineering.

Sullivan, D. A., 1981, "Historical review of real-fluid isentropic flow models.", J. Fluids Eng., Vol. 103.

Thompson, K. W., 1987, "Time dependent boundary conditions for hyperbolic systems.", J. Comput. Physics., Vol. 68, pp. 1-24.

Williamson, J. H., 1980, "Low-storage Runge-Kutta schemes.", J. Comput. Physics., Vol. 35, pp. 48-56.

## 8. Responsibility notice

The author(s) is (are) the only responsible for the printed material included in this paper